Vol. 3 • No. 10 • October • 2019
www.advsustainsys.com

# ADVANCED SUSTAINABLE SYSTEMS

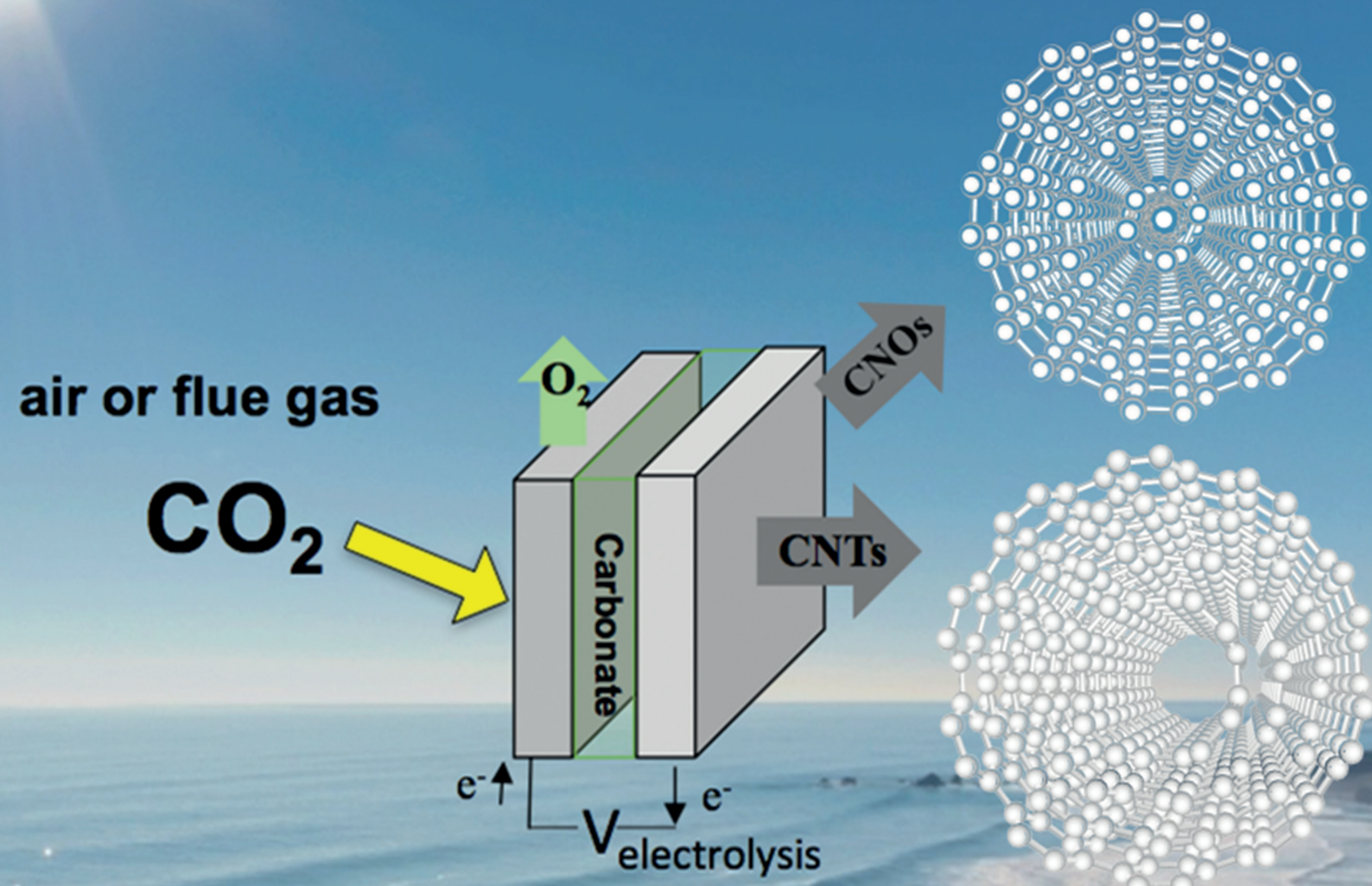


WILEY-VCH

ADVANCED SUSTAINABLE SYSTEMS

www.advsustainsys.com

# Carbon Nano-Onions Made Directly from $CO_2$ by Molten Electrolysis for Greenhouse Gas Mitigation

*Xinye Liu, Jiawen Ren, Gad Licht, Xirui Wang, and Stuart Licht**

**A high yield, low energy synthesis of carbon nano-onions (CNOs) by electrolysis of $CO_2$ in molten carbonate is presented. Carbon nano-onions are a recently recognized, less studied morphology of carbon nanomaterials consisting of nested concentric carbon spheroids. Previously, a high yield growth of carbon nanotubes by $CO_2$ electrolysis in molten carbonate was achieved through transition metal nucleation points on the electrolysis cathode. Here, effective low energy CNO synthesis from $CO_2$ is achieved instead by excluding those nucleating agents from the molten carbonate growth medium resulting in a profusion of uniform CNOs, with an increasing diameter correlated to increasing growth time. $CO_2$ transformation to valuable materials, such as CNOs, adds value to $CO_2$ to incentivize consumption of this greenhouse pollutant. For example, CNOs are currently valued 20 000 times higher than coal.**

## 1. Introduction

A new high yield, low energy chemistry that produces carbon nano-onions (CNOs) from carbon dioxide is presented here providing impetus for production of this valuable product to mitigate this greenhouse gas. As illustrated in **Figure 1**, the transformation of $CO_2$ to CNOs shown here can use concentrated $CO_2$ as found in flue gas, or directly from air (direct air carbon capture, without the need to preconcentrate the $CO_2$). $CO_2$ is bubbled into a molten carbonate and split by electrolysis, and the moltenate carbon has a high affinity for $CO_2$ absorption.

$CO_2$ use and conversion to valuable materials such as CNOs, currently valued over a $1 million per ton, adds value to $CO_2$ to incentivize use of this greenhouse gas pollutant. Due to synthetic complexities, CNOs are only available in small quantities, but this value is 20 000 fold higher than the price of power plant coal. The interactive dynamics of the land, sea, and atmosphere are complex, but even by the 1800's the thermal insulating, greenhouse gas warming properties of $CO_2$ were well established and by 1896 Nobel laureate Arrhenius (physicist, chemist, and electrolytic theorist) estimated the greenhouse effect magnitude and wrote in 1908 in the Worlds in the Making: "any doubling of the percentage of carbon dioxide in the air would raise the temperature of the earth's surface by 4 °C; ... The enormous combustion of coal by our industrial establishments suffices to increase the percentage of carbon dioxide in the air to a perceptible degree."[1]

Coal is valued at $40 to $60 per ton. However, other forms of solid carbon such as graphite are valued at over $1000 per ton or more. Due to the high cost of Chemical Vapor Deposition (CVD) synthesis another morphology of solid carbon, carbon nanotubes are valued at over $100 000 per ton, and CNOs are valued even higher due to the higher cost of production, such as the carbon nano-diamonds precursor used in their high temperature pyrolysis syntheses. If these materials can be synthesized from carbon dioxide, rather than organometallics or nano-diamonds at low energy, low cost and low carbon footprint, then they provide a powerful economic impetus to consume the greenhouse gas carbon dioxide. Here, an alternative chemistry of carbon nano-onion synthesis is presented. This opens a path to a decrease in CNO synthesis cost providing impetus for their application.

Carbon nano-onions are a less studied morphology of carbon nanomaterials consisting of nested concentric carbon spheroids. The first observation of the structures appears to have noted by Iijima in 1980,[2] and the first synthesis by Ugarte in 1992 using intense electron-beam irradiation of soot.[3] Studies variously refer to this carbon morphology as onion-like structures, carbon nano-onions, carbon onions, carbon spheres, or nested fullerenes. Carbon nano-onions have a range of remarkable applications, but these applications have been largely ignored due to their high synthesis cost. Closely related morphologies of molybdenum and tungsten diselenide nested fullerenes and their lubrication properties have driven sales of thousands of tons per year of these alternative inorganic fullerenes.[4] Carbon nano-onion applications often focus on the confined, high surface area of chargeable surfaces or symmetry of the CNO morphology. Examples include nano-onion ultrahigh power super capacitors with unusually high charge storage due to the ease with which ions can access the active material,[5] maximum anodic capacity lithium batteries,[6,7] increased capacity gas, and energy storage materials with a high 984.3 $m^2\ g^{-1}$ specific area,[8] increased activity in heterogeneous catalysis such as for styrene oxidative dehydrogenation

X. Liu, Dr. J. Ren, G. Licht, Dr. X. Wang, Prof. S. Licht
Department of Chemistry
George Washington University
Washington, DC 20052, USA
E-mail: slicht@gwu.edu

The ORCID identification number(s) for the author(s) of this article can be found under https://doi.org/10.1002/adsu.201900056.

**DOI: 10.1002/adsu.201900056**

 

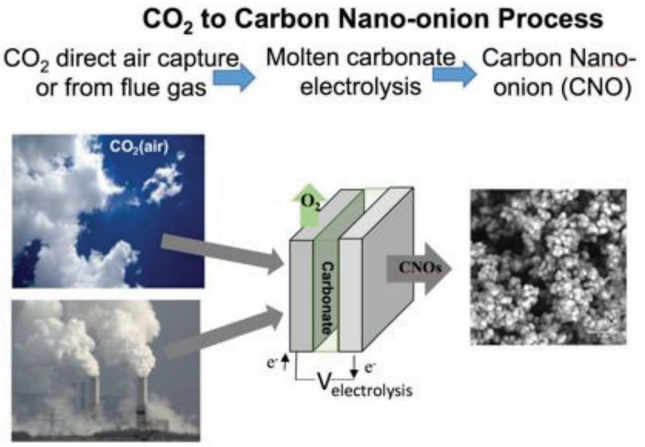


**Figure 1.** High yield electrolytic synthesis of carbon nano-onions from $CO_2$, either directly from the air or from smoke stack $CO_2$, in molten carbonate.

of ethylbenzene to styrene,[9] and CNOs were employed as the support for Pt in direct methanol fuel cells outperforming Pt/Vulcan XC-72 in the electro-oxidation of methanol.[10] Balancing symmetry and defects with high conductivity facilitates CNOs use as effective electromagnetic shielding provides efficient attenuation of the EMF spectrum from 12 to 203 THz,[11] and strong optical limiting action with negligible nonlinear refraction.[12] Biomedical applications have also been investigated,[13] and functionalized[14] and larger CNOs have been demonstrated to support high pressure before fracture, and demonstrated for aqueous-based lubrication as "ball bearings."[15]

Carbon nano-onions can be produced in gram-scale quantities by treatment of commercially available nanodiamonds or by the combustion of naphthalene[14,16] or by CVD (catalytic and noncatalytic).[17,18] Various synthesis methodologies have been reviewed; gram per hour quantities were obtained by high energy laser excitation of ethylene.[19,20] Other methodologies include ball milling,[21,22] and arc discharge between graphite electrodes.[23] Carbon nano-onions can also be synthesized using arc discharge, laser ablation and plasma processes, shock compression techniques, autoclave processes (catalytic and noncatalytic), and by carbonization routes,[24] thermal pyrolysis of alcohol at high 2700 K,[25] and high fluence 120 keV implantation of carbon ions into copper and silver.[26]

According to a recent review, thermal detonation anneal of nanodiamond powders has emerged as the most practical method for producing carbon nano-onions with a pricing that needs to include the ≈$2.4 million per ton price of the nanodiamonds precursor.[6] Challenges to the bulk production of bulk carbon nano-onions has limited their commercial availability. A producer sells 40±20 nm quasi spherical carbon nano-onions in gram quantities at a ton extrapolated price of $195 million per ton (including the academic discount),[27] another sells 37±7 nm carbon onions with 50–55 concentric layers with an extrapolated price (from 0.1 g units sold) of $3350 million per ton.[28]

Multiwalled carbon nanotubes (CNTs) comprised of concentric cylinders of graphene sheet have been studied in greater detail than their analogous CNO concentric spheroid counterparts CNOs. In 2015 we introduced a chemistry to synthesize CNTs at high yield by electrolysis of $CO_2$,[1,29–33,35–39] rather than their conventional CVD synthesis from organometallics. We have demonstrated[31] and quantified[39] the affinity for molten lithium carbonates to absorb both atmospheric and flue gas levels of $CO_2$, and have previously utilized $^{13}C$ isotope $CO_2$ to track and demonstrate in molten lithium carbonate that $CO_2$ originating from the gas phase serves as the renewable carbon building blocks in the observed CNT product and the net reaction is in accord with[31]

$$\text{Dissolution}: CO_2\,(\text{gas}) + Li_2O\,(\text{soluble}) \rightarrow Li_2CO_3\,(\text{molten}) \quad (1)$$

$$\text{Electrolysis}: Li_2CO_3\,(\text{molten}) \rightarrow C\,(\text{CNT}) + Li_2O\,(\text{soluble}) + O_2\,(\text{gas}) \quad (2)$$

$$\text{Net}: CO_2\,(\text{gas}) \rightarrow C\,(\text{CNT}) + O_2\,(\text{gas}) \quad (3)$$

We presented the low energy electrolytic splitting of $CO_2$ to either carbon nanofibers and nanotubes by molten lithium carbonate electrolysis, and demonstrated that the less expensive natural carbon isotope mix ($^{12}C_{0.99}{}^{13}C_{0.01}O_2$, rather than $^{13}CO_2$) produced the more expensive carbon nanotube, rather than nanofiber product,[30,31] and also that CNTs are formed at high yield not only in pure $Li_2CO_3$, but also in mixed Li/Na, and Li/Ba and/or Ca molten carbonate electrolytes.[32,33] A study of 5–10% $Li_2CO_3$ in molten chloride had previously concluded that "production of CNTs and nanofibers by electrolysis in molten lithium carbonate is impossible "because" reduction and carbon deposition occurred by Li discharge and intercalation into the cathode."[34] That assessment was correct, but did not anticipate the alternative transition metal nuclei growth mechanism paths from molten $Li_2CO_3$ observed here (including the new multitransition metal facilitated pathway).

We have introduced and studied the high yield, molten carbonate electrolytic transformation of $CO_2$ to CNTs (referred to as the "C2CNT") process' applicability to transforming $CO_2$ from the flue gas of fossil fuel power or cement plants to carbon nanotubes.[35,36] High yield, low electrolysis voltage, and high uniformity CNTs were demonstrated to be produced from dissolved $CO_2$ in a variety of alkali and alkali-earth carbonate electrolytes,[32,33] and straight (low defect) or tangled (high defect) were controlled through the addition or exclusion of oxide added to the molten carbonate electrolyte.[29,32,33,37] A variety of cathode substrates were studied as effective for the C2CNT process, and we demonstrated that very long (mm length) CNTs can be grown, and/or high conductivity CNTs, such as boron and other doped CNTs are readily formed by the controlled addition of impurities to the electrolyte during the electrosynthesis.[1,33,38]

In this study we provide for the first time an exploration of the initial phases of molten carbonate electrolysis CNT growth showing their relevance to discovery and introduction here of an alternative high yield carbon nano-onion synthesis:

$$\text{Electrolysis}: Li_2CO_3\,(\text{molten}) \rightarrow C\,(\text{CNO}) + Li_2O\,(\text{soluble}) + O_2\,(\text{gas}) \quad (2a)$$

$$\text{Net}: CO_2\,(\text{gas}) \rightarrow C\,(\text{CNO}) + O_2\,(\text{gas}) \quad (3a)$$

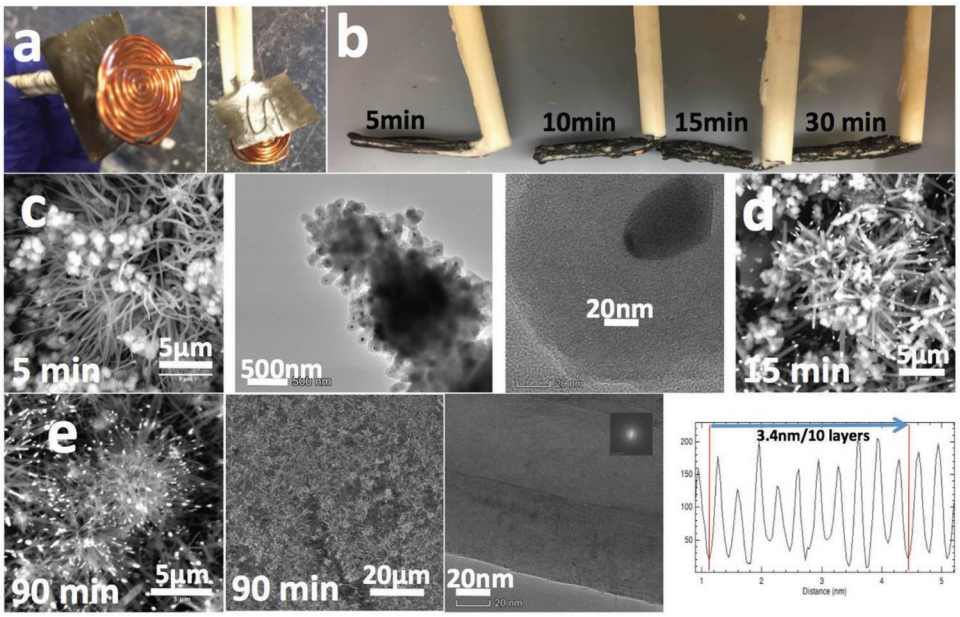


**Figure 2.** Transition metal on cathode facilitated $CO_2$ electrolysis in molten carbonate drives carbon nanotube growth. a) Ir/Pt anode and copper cathode (prior to Ni powder application) before electrolysis. b) the extracted, washed cathode product after constant 0.2 A $cm^{-2}$ electrolyses of various durations in 770 °C $Li_2CO_3$. c) SEM and TEM of the product after 5 min of electrolysis and d) SEM after a 15 min electrolysis. e) SEM and TEM of the product after 90 min of electrolysis. Bottom right: interspatial graphene layer between the individual CNT walls in the adjacent TEM.

## 2. Results and Discussion

### 2.1. $CO_2$ to CNT over CNO as a Preferred Morphology in the Presence of Ni Nucleation

This section studies the earliest phases of C2CNT carbon nanotube growth for comparison to differences observed in the CNO growth in the next section. In the presence of transition metal nucleation agents such as nickel and chromium, we have demonstrated the controlled growth of carbon nanotubes from $CO_2$ as it is dissolved in a molten carbonate electrolyte.

The carbon nanotube growth has been demonstrated on a variety of cathodes (steel, copper, nickel, graphite, brass, and a variety of other alloys).[1,29–33,37–39] Nickel and nickel alloys form a thin, stabilizing oxide layer when used as an anode, and the net reaction is the four electron reduction of $CO_2$ to form the building block carbons of CNTs. During electrolysis, a carbon product accumulates at the cathode and oxygen evolves at the anode in accord with a $CO_2$ splitting reaction. We have shown that a variety of inorganic carbonates are effective for this electrolysis.[1,29–33,37,38]

In the first series of experiments, a stable highly insoluble 5 $cm^2$ Ir/Pt foil is used as an anode to minimize dissolution of metal cations and a coiled copper wire with exposed surface area 5 $cm^2$ is horizontally adjacent and 1 cm under the anode (as shown in **Figure 2**a). Copper is chosen as the cathode for its previously demonstrated tendency to grow short, small CNTs.[38] The nucleation metal, nickel, is specifically added by spreading and drying an aqueous paste of 0.2 g of 3 to 7 µm Ni powder and 0.1 g of DI water over the upper surface of the cathode. The electrode assembly is placed in 50 g of 770 °C $Li_2CO_3$ (melting point 723 °C) and electrolyzed for a short duration of from 5 to 90 min at 1 A (0.2 A $cm^{-2}$) within a 100 mL alumina crucible. After each successive electrolysis, the cathode is cooled, the Figure 2b black cathode product is removed, cleaned by acid to remove solidified electrolyte and weighed. The electrolysis coulombic efficiency is calculated from the measured product mass divided by the theoretical mass of carbon from the product of the time and current (four electrons per carbon). This coulombic efficiency averages 97% for these electrolyses. For example, the 90 min synthesis yields 0.163 g, rather than 0.168 g carbon based on 1A x 5400 s, 1 mol e- per 96 485 As, $n = 4$ e- reduction, and 12.01 g carbon $mol^{-1}$.

In the presence of nickel added as a nucleating agent, the initial 5 min of product growth as shown with SEM (scanning electron microscopy) and TEM (transmission electron microscopy), in the middle panel of Figure 2c, forms both quasi-spherical (spheroid) and open-core nanotubes, and under increasing TEM magnification the nanotubes appear to be forming from the less ordered quasispherical growths. The SEM and TEM in the middle focus on the nickel (by EDS) nucleation point visible at the tips of nanotubes extending outward from the spheroids during the first 5 min of electrolytic growth at the cathode. Figure 2d,e shows the increasing dominance of the carbon nanotube over the spheroid morphology as the ensuing electrolysis time increases from 15 to 90 min. The individual walls of the multiwalled carbon nanotube are evident by TEM in the right lower side of Figure 2e with graphite layers separated by a grapheme–graphene layered typical spacing of 0.34 nm. **Figure 3** presents an expanded TEM view showing the individual layering of the concentric carbon nanotube walls, as well as the increasing number of nanotube walls with electrolysis time. The tapered CNT morphology observed after 5 min of electrolysis in Figure 2c, resolves into a uniform cylindrical shape observed with increasing electrolysis time, and the averaged CNT diameter increases respectively with 5, 30, and

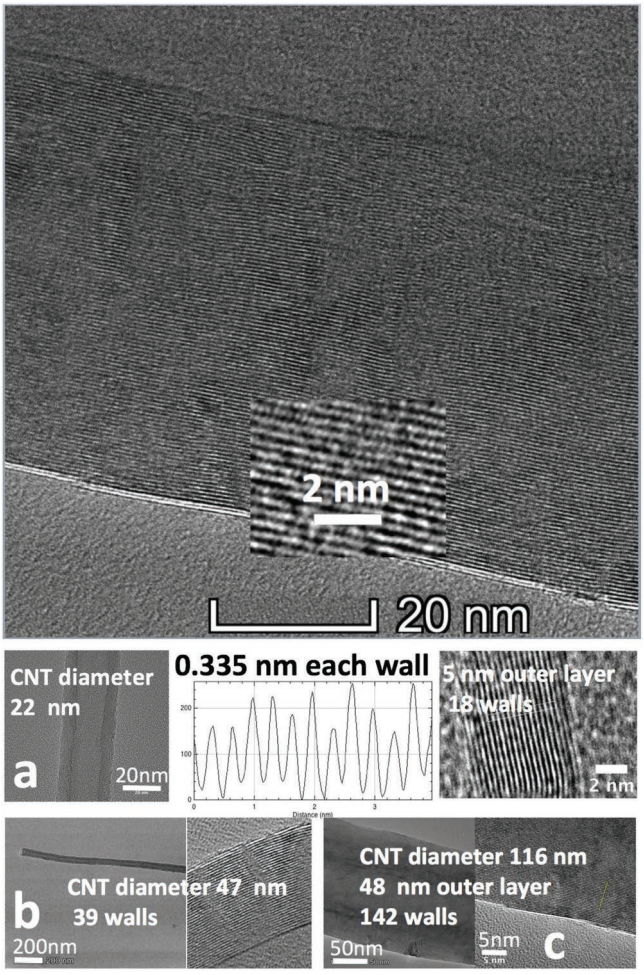


**Figure 3.** Carbon nanotube walls in molten carbonated synthesized CNTs. Top: an expanded view of the Figure 2, row c, 20 nm scale bar panel of the carbon nanotube product after 90 min synthesis. The synthesis is by electrolysis in 770 °C $Li_2CO_3$ at a 5 $cm^2$ coiled copper wire Ni powder). The synthesis produces a pure CNT product whose diameter increases with electrolysis time. TEM of the synthesis product subsequent to a) 15, b) 30, or c) 90 min electrolysis.

90 min of electrolysis time. The 90 min electrolysis contains the highest concentration of CNT (and the lowest concentration of spheroids) in the product; the CNTs have length varying from 4 to 7 μm. As seen in the Figure 2e, the CNTs spread out from a variety of central foci consistent with a root mechanism of growth. In the root mechanism nucleation points act as stationary bases for CNT growth.

As indicated in **Figure 4**, transition metal nucleating agents that promote CNT growth may also be added indirectly to the molten carbon electrolysis cell. For example, when the anode is composed of a less noble metal than iridium, during the initial formation of catalytic stabilizing oxide layer on the anode surface (such as nickel oxide from a nickel anode, or nickel chromium oxide from Nichrome) oxidized transition metal species are released to the electrolyte. These species upon reduction at the cathode can serve as effective CNT nucleation points; rather than nickel powder directly on the cathode as demonstrated in the Figure 2 series of electrolyses. In Figure 4 an electrolysis cell is configured with 5 $cm^2$ coiled using a Nichrome wire anode and a coiled Monel (nickel copper based alloy) wire cathode. No other nucleating agent (no nickel powder) is added to the cell. We have previously shown both Ni and Cr released from the anode, as well as the Monel cathode substrate, promote the growth of long, high aspect (length/diameter) ratio carbon nanotubes, a "CNT wool" product.[1] As in the analogous CVD growth, we observe in C2CNT that Ni promotes CNT growth and Cr promotes CNT repair providing a molten carbonate electrolysis medium to grow long CNTs.[1] As illustrated in Figure 4c, carbon nanotubes in molten carbonate can grow from either a tip (left) or base (root) transition nucleation growth mechanism. In Figure 4b, the cooled, washed, peeled (from the Monel cathode) CNT wool product shows evidence of multilayered graphene next to the cathode, followed by increasing ordered tip based growth of long CNTs.

We hypothesize that conditions which inhibit stability of the nucleation points during molten carbonate electrolyses will also inhibit formation of the C2CNT carbon nanotube product. The electrode product subsequent to current oscillations is studied in **Figure 5**. Two 9 $cm^2$ planar Ni200 electrodes (Nickel 200: >99% Ni and <0.15% C) electrodes, shown in Figure 5a subsequent to cycling, were cycled at +0.5A and −0.5A thrice per hour for 4 h in 770 °C $Li_2CO_3$. This cyclically reverses the measured cell bias (Figure 5a right side). Subsequent to electrolysis, the electrodes are inspected by EDS and SEM. The majority of the area is composed of nickel, with smaller areas of nickel oxide (Figure 5b) and additionally spheroid carbon deposits are observed (Figure 5c). Experimental constraints which maximize this observed carbon spheroid product are explored in the next section.

### 2.2. Probing $CO_2$ to Carbon Nano-Onion Transformation in Molten Carbonate

Using isotopic $^{13}C$ (gas phase $^{13}CO_2$) tracking, we have previously demonstrated that gas phase carbon dioxide provides the basic carbon building block source for the carbon products grown on the cathode during electrolytic $CO_2$ splitting in molten carbonate electrolysis.[31] In all experiments in this study, the heated electrolysis cell is open to the air providing sufficient $CO_2$ (at ≈415 ppm) from the air. At the lower current densities employed in this study, this direct air carbon capture of $CO_2$ is sufficient to continuously renew the electrolyte. At higher current densities (>0.2A $cm^{-2}$) than those explored in this study, we have shown that bubbled $CO_2$ or flue gas is needed to prevent the carbonate electrolyte from being partially consumed during the carbon product electrolysis, and that during the electrolysis sufficient heat is generated through the $CO_2$ solvation, reaction 1, and electrolysis overpotential to heat the insulated electrolysis (external heating is not required in an insulated cell subsequent to initiation of the electrolysis).[39] In creating an electrolytic molten carbonate environment conducive to formation of a carbon spheroid produce nickel powder was not added and an Ir/Pt anode was used to inhibit nickel or chromium nucleation or growth of the carbon nanotube morphology.

While electrolysis in 770 °C $Li_2CO_3$ generated the desired spheroid product at the anode, the product was a mix of

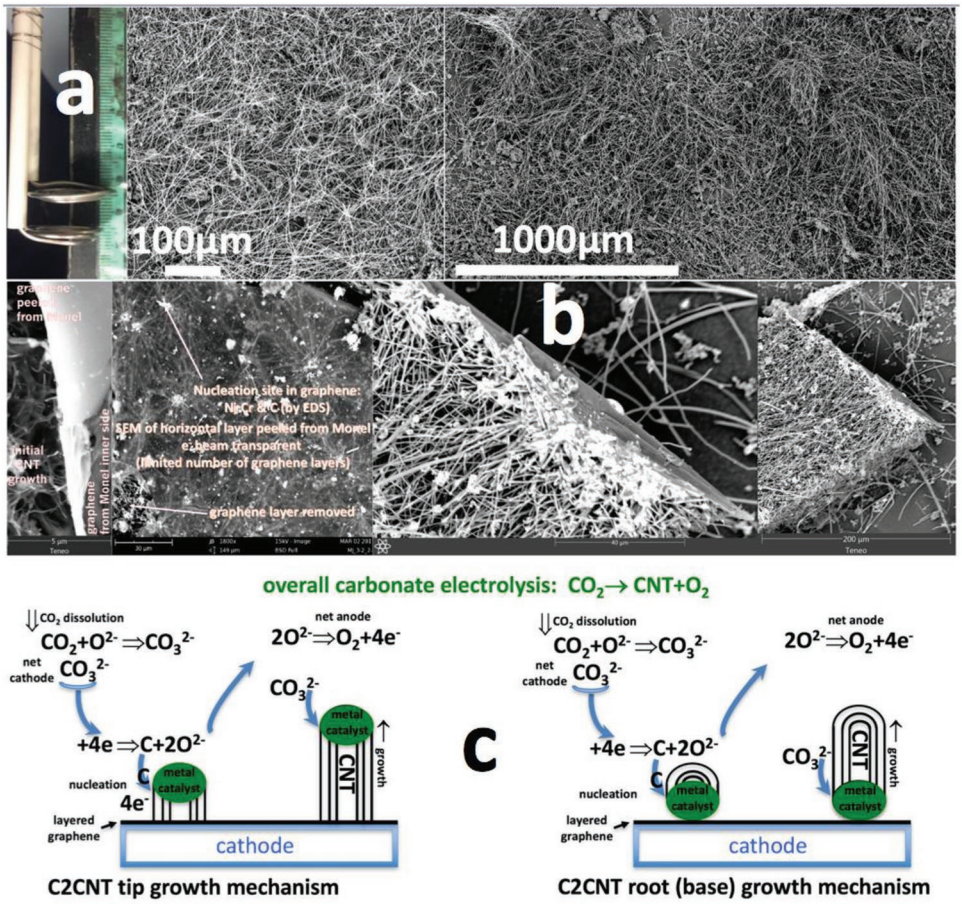


**Figure 4.** Long carbon nanotube "wool" grown during extended (18 h electrolysis) at a constant electrolysis 0.1 A $cm^{-2}$ current density between 5 $cm^2$ Nichrome anode and Monel coiled wire anodes a) separated by 1 cm in 50 g of 770 °C $Li_2CO_3$ (heated 24 h prior to electrode immersion). Modified from reference 1. a) Copper cathode and Ir/Pt electrodes before electrolysis and the extracted cathode product subsequent to various duration constant 0.2 A $cm^{-2}$ electrolyses in 770 °C $L_2CO_3$. b) SEM and TEM of the product after 5 min of electrolysis. c) Proposed tip and root CNT growth mechanism by electrolytic splitting of $CO_2$ in molten cartbonate.Tip growth appears consistent with 4b product and base growth with 2e CNT product.

morphologies including carbon nanoribbons and "peapod" shaped morphologies. We have previously used an increasing, stepped constant "pre-electrolysis polarization to improve nanoproduct uniformity during molten carbonate electrolysis,[29] and here we use increasing steps current of 0.05A and 0.1A each for 10 min and 0.2A and 0.4A for 5 min each ($J$ = 10, 20, 40, and 80 mA $cm^{-2}$), prior to the start of a 90 min constant 1 A ($J$ = 200 mA $cm^{-2}$) electrolysis to promote carbon deposition. While zinc melts at a temperature below that of the electrolyte (Zn melts at 420 °C) and hence does not appear to act as a nucleation metal act in high temperature molten carbonate melts,[29] we have shown that it tends to encourage initial carbon deposition on the cathode.[29,40] Hence in order to promote carbon growth in the CNO syntheses, the pure copper coiled wire cathode used in Figure 2 is replaced with a galvanized steel (zinc metal coated steel) coiled wire cathode. Furthermore, addition of a high concentration of $Li_2O$ (5.9 moles per kg $Li_2CO_3$) resulted a "pure" (>90%) carbon spheroid cathode product as shown in **Figure 6**b. We have previously shown that lithium oxide addition to the electrolyte results in curved, rather than straight carbon nanotube growth, increasing ($sp^3$) defects in the flat, layered $sp^2$ morphology .[29,39] This oxide-rich, nickel powder-free medium media encourages curvature and also minimizes nucleating transition metals to inhibit carbon nanotube growth and to enhance carbon spheroids as a preferred product morphology. These oxide rich, Zn mediated, stepped "pre-electrolysis" conditions were used in subsequent carbon spheroid product syntheses.

The top portion of Figure 6 compares the carbon product synthesized over time with (a) and without (b) added nickel. When nickel is not added (bottom) the initial spheroid product (left) becomes a distinct carbon nano-onion morphology over time (middle and right). When nickel is added (6a) the initial mix of spheroids and tapered nanotubes develops into a distinct, uniform CNT product over time. In both cases, the electrolytic conditions are similar (770 °C, $Li_2CO_3$ electrolyte, 0.2 A $cm^{-2}$ constant electrolysis current density, planar Ir/Pt anodes and coiled wire cathodes electrolyte (either Cu Figure 6a, or galvanized steel Figure 6b) are used in 770 °C electrolyte (either pure $Li_2CO_3$ Figure 6a, or mixed with 5.9 m dissolved $Li_2O$ Figure 6b). EDS of each of CNO samples (synthesized without added nickel) indicate each is over 99% carbon. We do not observe residual electrolyte in the washed product, but should note the Phenom EDS does not have sufficient resolution

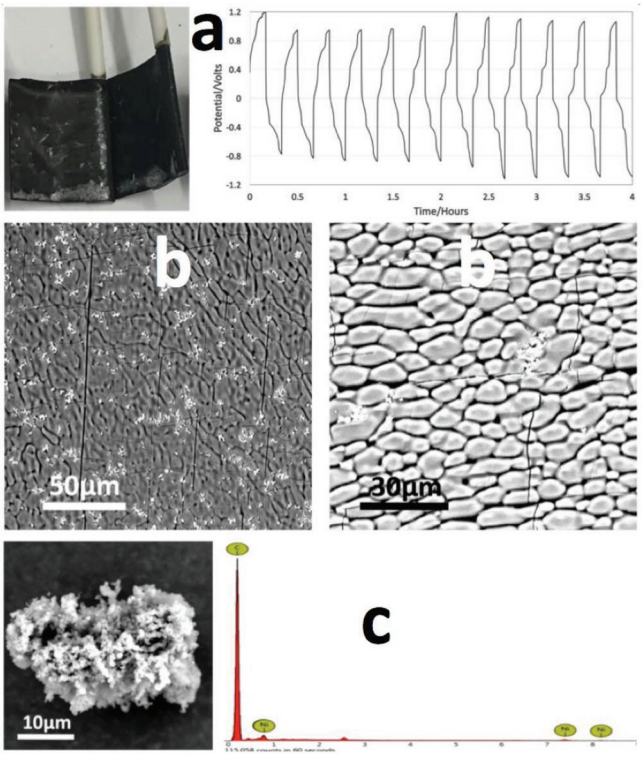


**Figure 5.** a) 9 $cm^2$ planar Ni 200 sheet after cycling the current from +0.5A to –0.5A thrice per hour for 4 h in 770 °C $Li_2CO_3$. b) SEM (shown) and EDS (not shown) exhibiting a majority of nickel with areas of nickel oxide coating (white spots), as well as c) carbon deposits (left). EDS of the carbon deposit (right).

to analyze for lowest (lithium) atomic weight elements (i.e., lithium).

The bottom portion of Figure 6b presents an overview (lower magnification SEM) of the variations syntheses presented (at higher magnification) in the middle panels of Figure 6b. In each case the product is a highly uniform diameter carbon spheroids. Not evident, in these low magnification SEM and as shown in subsequent figures i) each of the spheroids in the second row of Figure 6 is in turn formed from clusters of nano-onions and ii) the nano-onion morphology is indistinct in the initial (first 5 min), and iii) evolves to a morphology of structured concentric buckyballs with longer duration syntheses; this will be explored in Figures 8–10.

With increasing CNO synthesis time, Raman shift indicates an increasing height of the 1580 $cm^{-1}$ (G band) relative to the 1350 $cm^{-1}$ (D band) (as exemplified in **Figure 7** for the 30 min synthesized CNOs along with their XRD); this indicates an increasing dominance of the high frequency $E_{2g}$ first order mode (G band) and the disorder-induced mode (D band) reflecting the increasing $sp^2$ compared to $sp^3$ character of the concentric spheroid morphologies; the other Raman of the other syntheses are similar, but lower with G band/D band with shorter synthesis time.[14] The XRD observed at 2 theta = 26.3° is typical of a graphitic allotrope diffraction peak and the thin width is indicative of a high degree of crystallinity.

To probe the intermediate stage of mixed CNT/CNO cathode growth during molten carbonate synthesis, minimal nickel was included in the otherwise nickel-free electrochemical environment and introduced during the synthesis by use of a nickel crucible during the electrolysis and a stepped as previously mentioned in section 3.2 "pre-electrolysis" condition, 90 min electrolysis performed. High resolution SEM of the interfacial mixed CNT/CNO-onion cathode is shown in **Figure 8**, and it is apparent that the larger spheroids are composed of bundles of smaller nanomaterials. TEM of the same 5 and 30 min duration electrolyses in the bottom portion of Figures 7 and 8, exhibit large bundles as well as smaller fragments; the latter are used to distinguish crystallinity of the samples by TEM. Figure 9 presents TEM of carbon nano-onion synthesis product after 5 min of molten carbon carbonate electrolysis under carbon spheroid producing conditions (without added Ni and in 770 °C $Li_2CO_3$ containing 5.9 m $Li_2O$ electrolyte), while Figure 10 presents TEM of the CNO product after 30 min of electrolysis. The 5 min duration electrolyses do not exhibit distinct graphene layers, whereas the longer duration electrolyses exhibit distinct concentrically increasing diameter spheroid morphology with a graphitic 0.35 nm interlayer separation.[31] The separated, as well as individual bundled nano-onions in the spheroids, have an increasing average diameter, as measured by ImageJ SEM automated optical counting software respectively after 5, 30, and 90 min of electrolysis of ±10, 66±6, and 96±2 nm, while the spheroids (bundled nano-onions) have a combined ten-fold higher diameter of ≈400, 600, and 900 nm as seen in Figure 6b. We reiterate that while the short duration (5 min) electrolysis formed nano-onions have a distinctive size as seen in the left side of **Figure 9**, unlike the longer duration syntheses the product after 5 min does not yet exhibit the distinctive concentric spherical graphene shells evident in **Figure 10**.

The morphological effect of increasing crystallinity with increasing electrolysis time observed in Figures 9 and 10 appear to be analogous to the effect of increasing crystallinity with increasing pyrolysis temperature as observed by Zeiger et al. and reprinted in **Figure 11**. This similarity of growth mechanism is despite very different physical chemical media (molten electrolysis vs high temperature pyrolysis) and with very different reactants ($CO_2$ vs nanodiamonds).

As shown in the SEM **Figure 12**, the dissolution of additional low levels of zinc to the electrolyte as ZnO (0.06 molal ZnO) does not appear to affect the spheroid morphology of the carbon product, and this stands in stark contrast to the addition of low levels of nickel, chromium, iron, or copper oxides which tend to promote other carbon nanomorphologies such as carbon nanotubes. As seen in **Figure 13**, extended electrolyses (15 h, rather than 1.5 h) produces more, but not significantly larger, carbon nano-onions.

### 2.3. Brief Economic Assessment

With the exception of the noble-metal anode, all components of the molten carbonate electrolytic transformation of $CO_2$ to carbon nano-onions are inexpensive. As delineated in our recent carbon nanotube synthesis study molten carbonate $CO_2$ electrolysis costs are analogous to, and less expensive than the materials, capital, and labor costs for the industrial production of aluminum from another oxide (bauxite, rather

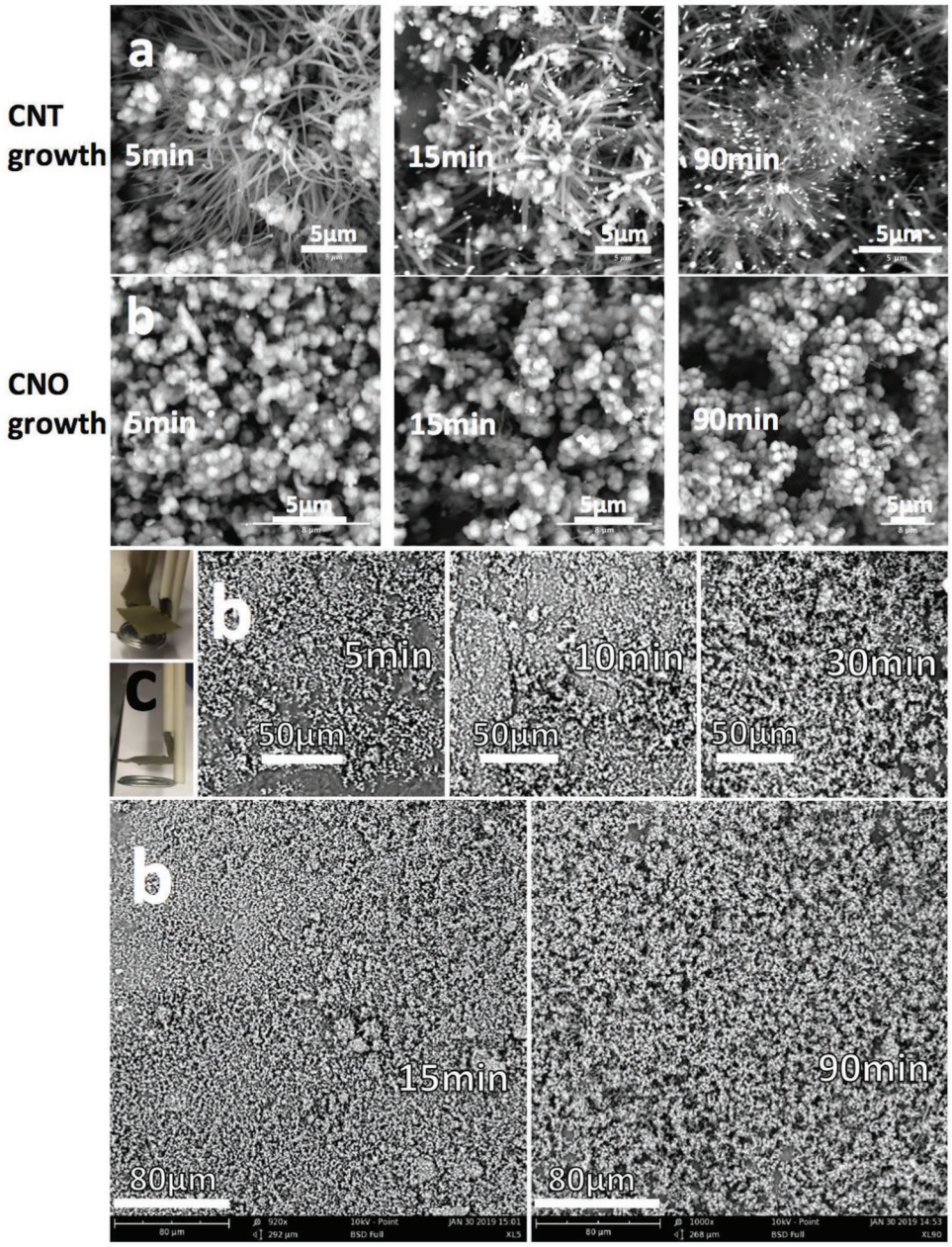


**Figure 6.** SEM comparison of the carbon product synthesized in time with, a) and without, b) added nickel. When nickel is not added (bottom) the initial spheroid product that is evident becomes a distinct carbon nano-onion morphology over time. When nickel is added (a) the initial mix of spheroids and tapered nanotubes develops into a distinct, uniform carbon nanotube product over time. (b) High yield carbon nano-onion synthesis. SEM of the washed cathode product after various duration electrolyses. Each product contains a high yield of uniform pure carbon spheroids. c) 5 $cm^2$ Ir/Pt anode and the coiled galvanized steel wire cathodes before the (b) syntheses: 0.2 A $cm^{-2}$ electrolysis in 770 °C $Li_2CO_3$ containing 5.9 m $Li_2O$.

than carbon dioxide).[1,38] As previously described $CO_2$ electrolytic splitting in molten carbonates process bears many similarities to aluminum smelting. Both processes consist of molten electrolysis, and do not use noble or exotic materials.[38] Aluminum smelting produces aluminum metal from alumina (using bauxite, sodium hydroxide, and electricity), while C2CNT produces carbon nanotubes from carbon dioxide (using carbon dioxide and electricity). Aluminum smelting operates at 960 °C in a molten cryolite electrolyte. The C2CNT process operates under somewhat milder conditions at 770 °C in a less exotic, molten carbonate electrolyte. Both processes operate at high rate (hundreds of mA per $cm^2$) and low polarization. In both cases the electrolysis chamber consists of common metals, common insulators (such as kiln or "firebricks"), and control equipment. Electrolysis in the Aluminum smelting process is driven at ≈4 volts using three electrons per aluminum. The C2CNT electrolysis is driven at ≈1 volt using four electrons per carbon dioxide. C2CNT and aluminum smelters have approximately equivalent output (electrode area normalized mass/time) rates.

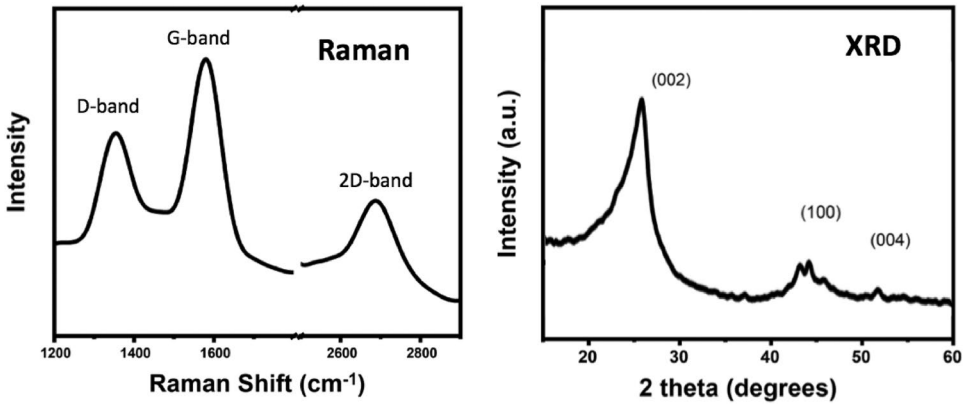


**Figure 7.** Raman (left) and XRD (right) spectra of the carbon nano-onion product by a 30 min molten carbonate synthesis (without added nickel) as delineated in the legend of Figure 6.

The noble iridium/platinum anode in this study is purposely used here to inhibit CNT formation and enhance the observed formation of the desired CNO product by preventing introduction from the anode, migration, reduction, and formation of nickel or chromium nucleation sites on the cathode which we demonstrated favored formation of the alternative CNT product in other studies.[1,29–40] However, an iridium or iridium alloy anode is not a prerequisite for high yield CNO growth. The inhibition of low levels of nickel migration from a nickel or nickel containing alloy anode, or a thin film iridium anode are readily envisioned and will be the topic of an ensuing study. Here, we reference some of the many relevant studies on thin film iridium deposition.[41–48]

Carbon nanotube synthesis by electrolysis of carbon dioxide in molten carbonate is readily scalable, and scales upward linearly with the surface area of the electrolysis electrodes,[29,39] facilitating the analogous larger scale synthesis of carbon nano-onions. 150 years ago aluminum was expensive with little market. However, via a change of chemical technology today aluminum is inexpensive with a mass market. The voltage for reduction of the carbon dioxide to carbon by reduction is in the 0.8 to 2 V domain,[30] whereas that for aluminum production is over 4 V. The molten carbonates used here are less noxious and operate at lower temperature than the cryolite-type electrolyte used in aluminum production (770 °C compared to 960 °C); the basic kiln components are similar and to an extent simpler than in aluminum production (CNO production by molten electrolysis does not use a consumable anode, whereas aluminum production does). The current market value of aluminum of ≈$1500 per ton sets a maximum cost to aluminum production costs. Hence, $1000 is a reasonable upper bound estimation to industrial carbon nano-onion production by carbon dioxide electrolysis, excluding anode costs to be determined, in molten carbonates. This cost is significantly lower than the current $1M+ value of CNOs, and may provide a significant incentive to use the greenhouse gas carbon dioxide as a reactant to produce carbon nano-onions. Assuming that mass markets for carbon nano-onions develop, this can provide a useful path forward to help break the anthropogenic carbon cycle to mitigate climate change.

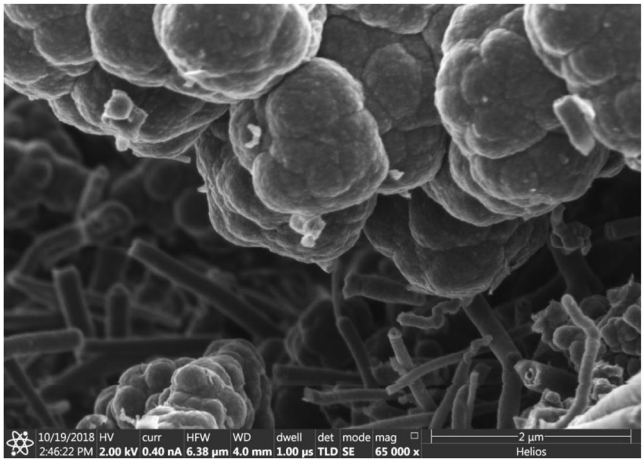


**Figure 8.** High resolution SEM of mixed carbon nanotube/nano-onion interface of washed cathode product subsequent to 0.2 A $cm^{-2}$ electrolysis between 5 $cm^2$ electrodes. The SEM has been slightly colorized to enhance contrast.

## 3. Conclusion

Here, we show a new high yield pathway to produce carbon nano-onions directly from atmospheric or exhaust $CO_2$ in an inexpensive molten electrolysis. CNOs are a more recently

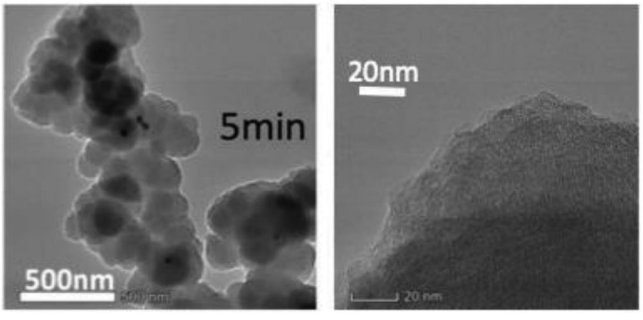


**Figure 9.** TEM of carbon nano-onion synthesis product after 5 min of molten carbon carbonate electrolysis (without added Ni and in 770 °C $Li_2CO_3$ containing 5.9 m $Li_2O$ electrolyte). The electrolysis conditions are detailed in the legend of Figure 6.

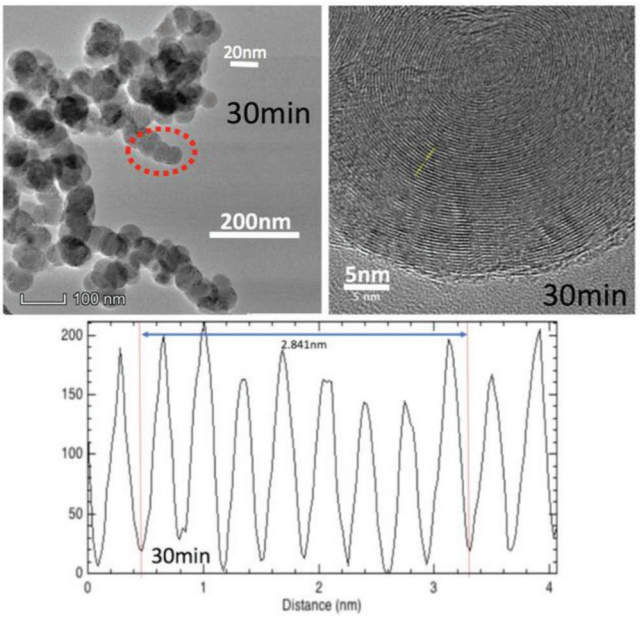


**Figure 10.** TEM of carbon nano-onion synthesis product obtained with 30 min of molten carbon carbonate electrolysis (at 770 °C, without added Ni, and with 5.9 m $Li_2O$ in the $Li_2CO_3$ electrolyte). The electrolysis conditions are detailed in the legend of Figure 6. Bottom: interspatial graphene layer between the individual CNT walls in the adjacent SEM.

recognized, less studied morphology of carbon nanomaterials consisting of nested concentric carbon spheroids. Formation of this highly valued, compact, readily stored form of carbon directly from carbon dioxide may provide a new pathway to mitigate this greenhouse gas. Today, carbon nano-onions production does not provide a path to consume the greenhouse gas $CO_2$, and utilizes synthetic processes that are several orders of magnitude more expensive such as pyrolysis of carbon nanodiamonds or chemical vapor deposition. We present the first high yield, inexpensive synthesis of carbon nano-onions from the direct electrolytic conversion of $CO_2$, dissolved in molten carbonates to CNOs at high rates using scalable, inexpensive cathodes. The CNO structure is tuned by inhibiting proximity of transition metals, such as nickel or chromium, which nucleate the formation of other carbon nanomaterial morphologies such as carbon nanotubes to allow dominant growth of the high yield CNO product. Effective high yield, low energy CNO

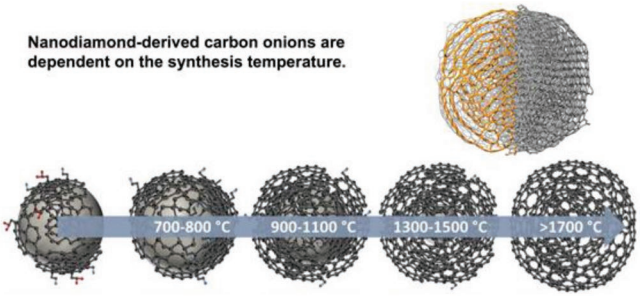


**Figure 11.** Synthesis of ordered carbon nano-onions by pyrolysis of nanodiamonds requires high temperature. Adapted with permission.[7] Copyright 2016, Royal Society of Chemistry.

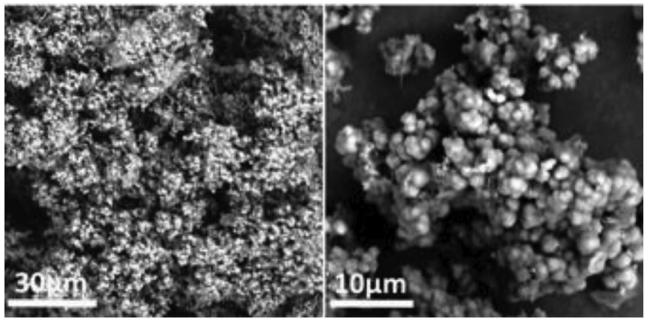


**Figure 12.** Added ZnO to the 770 °C electrolysis does not appear to affect the 1.5 h 0.2 A $cm^{-2}$ electrolysis carbon nano-onion product.

synthesis is achieved instead by excluding those nucleating agents from the molten carbonate growth medium resulting in a profusion of uniform CNOs, with an increasing diameter correlated to increasing growth time.

Applications for inexpensive CNOs include supercapacitors, battery anodes, and solid-lubricants. The geologic (graphite-like durability) stability of graphene allotrope carbon materials could provide a long-term repository to store atmospheric $CO_2$. SEM, EDS, and TEM characterization provides fundamental evidence of the high yield and purity of the CNO synthesis. The upper-bound estimate of the new chemistry of CNO production by molten carbonate electrolysis, excluding anode costs to be determined, of $1000 per ton, is several orders of magnitude less than alternatives. $CO_2$ use and conversion to valuable materials such as CNOs, currently valued over a $1 million per ton, adds value to $CO_2$ to incentivize use of this greenhouse gas pollutant. Future studies will explore inexpensive anodes for use in the $CO_2$ electrolytic growth of CNOs, and also explore application level material testing of the charge storage, electrochemical, and tribological properties of CNOs from $CO_2$.

## 4. Experimental Section

Electrolyses were driven galvanostatically in 50 g of 770 °C molten lithium carbonate (99% Alfa Aesar). The electrolysis was contained in a high form pure 100 mL alumina (AdValue 99.6%), or nickel (VWR) crucible. Cathodes were with copper or galvanized steel wires spiral

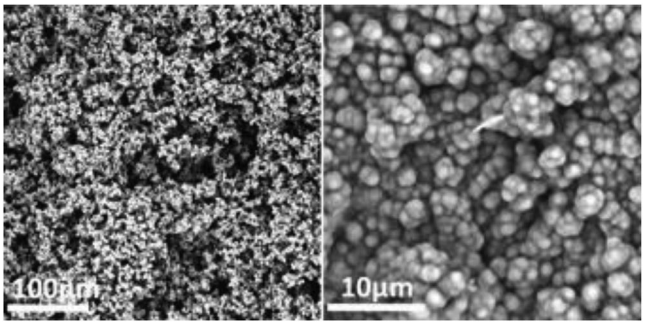


**Figure 13.** Extended duration (15 h), lower current 0.1 A $cm^{-2}$ electrolysis produces more, but not a significantly larger diameter carbon nano-onion product.

coiled to form a horizontal flat disc cathode of 5 $cm^2$. Area above this was a horizontal, square, planar 5 $cm^2$ Ir/Pt foil used as an anode. $CO_2$ or air flows freely into the cell; at low current densities air contains sufficient $CO_2$ to prevent the electrolyte loss during the electrolysis. Electrolyses were conducted at constant current at 770 °C in either pure $Li_2CO_3$ (Alfa Aesar 99%) or $Li_2CO_3$ with $Li_2O$ (Alfa Aesar 99.5%) as indicated.

During electrolysis, a carbon product accumulates at the cathode, which postelectrolysis easily peels off the extracted, cooled cathode. Electrolyte solidified with the product was removed by washing with either HCl or formic acid.[1] The former was quicker; the latter wash better preserves evidence of nucleating metals in the product. The washed carbon product was analyzed by PHENOM Pro-X Energy Dispersive Spectroscopy (EDS) on the PHENOM Pro-X SEM, or FEI Teneo LV SEM, FEI Helios FIB SEM, and by FEI Teneo Talos F200XTEM. Raman spectroscopy was measured with a LabRAM HR800 Raman microscope (HORIBA) using 532.14 nm wavelength incident laser light with a high resolution of 0.6 $cm^{-1}$. The synthesis yield, 100% x $C_{experimental}/C_{theoretical}$, was determined by the measured mass of washed carbon product removed from the cathode, $C_{experimental}$, and the theoretical mass, $C_{theoretical}$ = (Q/nF)x(12.01 g C $mol^{-1}$) which is determined from Q, the charge during the electrolysis, F, the Faraday (96 485 As $mol^{-1}$ $e^-$), and the $n$ = 4 e- $mol^{-1}$ reduction of tetravalent carbon. Expanded experimental details are in refs. [1] and [29].

## Acknowledgements

The authors are grateful to C2CNT for support of this research. Marcus Johnson under the direction of S.L. performed the Figure 5 experiment exhibiting low levels of the CNO product.

## Conflict of Interest

The authors declare no conflict of interest.

## Keywords

carbon dioxide electrolysis, carbon nanomaterials, carbon nano-onions, greenhouse gas mitigation, molten carbonate

Received: May 8, 2019
Revised: June 14, 2019
Published online:

[1] M. Johnson, J. Ren, M. Lefler, G. Licht, J. Vicini, X. Liu, S. Licht, *Mater. Today Energy* **2017**, *5*, 230.
[2] S. Iijima, *J. Cryst. Growth* **1980**, *50*, 675.
[3] D. Ugarte, *Nature* **1992**, *359*, 707.
[4] R. Tenne, A. N. Enyashin, *Nat. Nanotechol.* **2014**, *2*, 649.
[5] D. Pech, M. Brunet, H. Durou, P. Huang, V. Mochalin, Y. Gogotsi, P.-L. Taberna, P. Simon, *Nat. Nanotechnol.* **2010**, *5*, 651.
[6] F.-D. Han, B. Yao, Y.-J. Bai, *J. Phys. Chem. C* **2011**, *115*, 8923.
[7] M. Zeiger, N. Jackel, V. N. Mochalin, V. Presser, *J. Mater. Chem. A* **2016**, *4*, 3172.
[8] N. Sano, H. Wang, I. Alexandrou, M. Chhowalla, K. B. K. Teo, G. A. J. Amaratunga, K. Iimura, *J. Appl. Phys.* **2002**, *92*, 2783.
[9] N. Keller, N. I. Maksimova, V. V. Roddatis, M. Schur, G. Mestl, Y. V. Butenko, V. L. Kuznetsov, R. Schlogl, *Angew. Chem., Int. Ed.* **2002**, *41*, 1885.
[10] B. Xu, X. Yang, X. Wang, J. Guo, X. Liu, *J. Power Sources* **2006**, *162*, 160.
[11] O. Shenderova, V. Grishko, G. Cunningham, S. Moseenkov, G. McGuire, V. Kuznetsov, *Diamond Relat. Mater.* **2008**, *17*, 462.
[12] E. Koudoumas, O. Kokkinaki, M. Konstantaki, S. Couris, S. Korovin, P. Detkov, V. Kuznetsov, S. Pimenov, V. Pustovo, *Chem. Phys. Lett.* **2002**, *357*, 336.
[13] S. Giordani, A. Camisasca, V. Maffeis, *Curr. Med. Chem.* **2019**, *26*, https://doi.org/10.2174/0929867326666181126113957.
[14] J. Bartelmess, S. Giordani, *Beilstein J. Nanotechnol.* **2014**, *5*, 1980.
[15] J. E. St. Dennis, K. Jin, Vijay T. John, N. S. Pesika, *ACS Appl. Mater. Interfaces* **2011**, *3*, 2215.
[16] Y. M. Manawi, I. A. Samara, T. Al-Ansari, M. A. Atieh, *Materials* **2018**, *11*, 822.
[17] Y. Yang, X. Liu, X. Guo, H. Wen, B. Xu, *J. Nanopart. Res.* **2011**, *13*, 1979.
[18] M. Choucair, J. A. Stride, *Carbon* **2012**, *50*, 1109.
[19] L. Echegoyen, A. Ortiz, M. N. Chaur, A. J. Palkar, in *Chemistry of Nanocarbons* (Eds: T. Akasaka, F. Wudl, S. Nagase), John Wiley & Sons, Chichester, UK, **2010**, p. 463.
[20] Y. S. Zhou, W. Xiong, J. B. Park, *J. Laser Appl.* **2011**, *22*, 165604.
[21] J. Y. Huang, H. Yasuda, H. Mori, *Chem. Phys. Lett.* **1999**, *303*, 130.
[22] X. H. Chen, H. S. Yang, G. T. Wu, M. Wang, F. M. Deng, X. B. Zhang, J. C. Pen, W. Z. Li, *J. Cryst. Growth* **2000**, *218*, 57.
[23] N. Sano, H. Wang, M. Chhowalla, I. Alexandrou, G. A. J. Amaratunga, *Nature.* **2001**, *414*, 506.
[24] A. A. Deshmukh, S. D. Mhlanga, N. J. Coville, *Mater. Sci. Eng. R: Rep.* **2010**, *70*, 1.
[25] J.-C. Fan, H.-H. Sung, C.-R. Lin, M.-H. Lai, *J. Mater. Chem.* **2012**, *22*, 9794.
[26] T. Cabioc'h, M. Jaouen, E. Thune, P. Gúerin, C. Fayoux, M. F. Denanot, *Surf. Coat. Technol.* **2000**, *128–129*, 43.
[27] Graphitic Nano Onions LLC, http://graphiticnanoonions.com/ (accessed: January 2019).
[28] Carbon Onions (100 mg), https://market.carbonallotropes.com/home/3-carbon-onions-100-mg.html, (accessed: January 2019).
[29] J. Ren, F.-F. Li, J. Lau, L. Gonzalez-Urbina, S. Licht, *Nano Lett.* **2015**, *15*, 6142.
[30] J. Ren, J. Lau, M. Lefler, S. Licht, *J. Phys. Chem. C* **2015**, *119*, 23342.
[31] J. Ren, S. Licht, *Sci. Rep.* **2016**, *6*, 27760.
[32] H. Wu, Z. Li, D. Ji, Y. Liu, L. Li, D. Yuan, Z. Zhang, J. Ren, M. Lefler, B. Wang, S. Licht, *Carbon* **2016**, *106*, 208.
[33] J. Ren, M. Johnson, R. Singhal, S. Licht, *J. CO2 Util.* **2017**, *18*, 335.
[34] A. T. Dimitrov, *Maced. J. Chem. Eng.* **2009**, *28*, 111.
[35] J. Lau, G. Dey, S. Licht, *Energy Convers. Manage.* **2016**, *122*, 400.
[36] S. Licht, *J. CO2 Util.* **2017**, *18*, 378.
[37] S. Licht, A. Douglas, J. Ren, R. Carter, M. Lefler, C. Pint, *ACS Cent. Sci.* **2016**, *2*, 162.
[38] M. Johnson, J. Ren, M. Lefler, G. Licht, J. Vicini, Y. L. S. Licht, *Data Brief* **2017**, *14*, 592.
[39] S. Licht, arXiv, **2017**, 1710.07246 https://arxiv.org/abs/1710.07246.
[40] G. Dey, J. Ren, T. El-Ghazawi, S. Licht, *RSC Adv.* **2016**, *6*, 27191.
[41] N. V. Grushina, TI Saprykina, *J. Appl. Chem. USSR* **1992**, *65*, 2015.
[42] Y. Kamegaya, K. Sasaki, M. Oguri, T. Asaki, H. Kobayashi, T. Mitamura, *Electrochim. Acta* **1995**, *40*, 889.
[43] T. Ohsaka, Y. Matsubara, K. Hirano, T. Ohishi, *Int. J. Surface Eng. Coatings* **2007**, *85*, 260.
[44] T. Ohsaka, K. Hirano, S. Imabayashi, *Electrochem. Solid-State Lett.* **2010**, *13*, D65.
[45] B. Shuxin, Z. Li'an, Z. Hong, Y. Yicong, *Rare Metal Mater. Eng.* **2015**, *44*, 1816.
[46] S. S. Lopez, V. E. Cruz, J. A. Cobos-Murcia, M. A. Rodríguez, J. Avila. *Int. J. Electrochem. Sci.* **2015**, *10*, 9933.
[47] M. H. Allahyarzadeh, M. Aliofkhazraei, A. S. Rougaghdam, *Surf. Rev. Lett.* **2016**, *23*, 1630001.
[48] G. Sheela, M. Pushpavanam, S. Pushpavanam, *Int. J. Surface Eng. Coatings* **2017**, *8:5*, 191.

 